Walter P. Wolfe
Engineering Sciences Center
Sandia National Laboratories
Albuquerque, NM 87185-0836

Stuart S. Ochs
Aerospace Engineering Department
Iowa State University
Ames, IA 50011

CFD Calculations of S809 Aerodynamic Characteristics[1]

Steady-state, two-dimensional CFD calculations were made for the S809 laminar-flow, wind-turbine airfoil using the commercial code CFD-ACE. Comparisons of the computed pressure and aerodynamic coefficients were made with wind tunnel data from the Delft University 1.8 m × 1.25 m low-turbulence wind tunnel. This work highlights two areas in CFD that require further investigation and development in order to enable accurate numerical simulations of flow about current generation wind-turbine airfoils: transition prediction and turbulence modeling. The results show that the laminar-to-turbulent transition point must be modeled correctly to get accurate simulations for attached flow. Calculations also show that the standard turbulence model used in most commercial CFD codes, the k-ε model, is not appropriate at angles of attack with flow separation.

Introduction

In the design of a commercially viable wind turbine, it is critical that the design team have an accurate assessment of the aerodynamic characteristics of the airfoils that are being considered. Errors in the aerodynamic coefficients will result in errors in the turbine's performance estimates and economic projections. The most desirable situation is to have accurate experimental data sets for the correct airfoils throughout the design space. However, such data sets are not always available and the designer must rely on calculations.

In 1995, we began a limited investigation into the applicability of commercially available computational fluid dynamics (CFD) codes for calculating the aerodynamic characteristics of horizontal-axis wind-turbine airfoils. Because of the limited resources available, we had to limit our study to one CFD code and one airfoil section. In the following, we present the results to date from this study.

Airfoil Section

For this study, we chose an airfoil whose aerodynamic characteristics are representative of horizontal-axis wind-turbine (HAWT) airfoils, the S809. The S809 is a 21% thick, laminar-flow airfoil designed specifically for HAWT applications (Somers, 1989). A sketch of the airfoil is shown in Figure 1. A 600 mm-chord model of the S809 was tested in the 1.8 m × 1.25 m, low-turbulence wind tunnel at the Delft University of Technology. The results of these tests are reported by Somers (1989) and are used in this work for comparison with the numerical results. Another similarly sized model of the S809 was tested at Ohio State University. Our comparisons of the two experimental data sets showed that the results are essentially identical. In this paper, we do not show error bars on the experimental data since the original wind-tunnel data report does not provide error estimates.

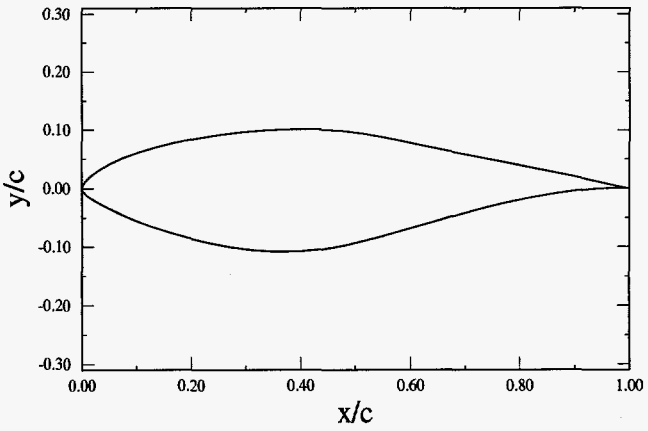

Figure 1. S809 Airfoil Profile

The experimental data show that at positive angles of attack below approximately 5°, the flow remains laminar over the forward half of the airfoil. It then undergoes laminar separation followed by a turbulent reattachment. As the angle of attack is increased further, the upper-surface transition point moves forward and the airfoil begins to experience small amounts of turbulent trailing-edge separation. At approximately 9°, the last 5% to 10% of the upper surface is separated. The upper-surface transition point has moved forward

[1] This work was supported by the United States Department of Energy under Contract DE-AC04-94AL85000.

DISCLAIMER

to approximately the leading edge. As the angle of attack is increased to 15°, the separated region moves forward to about the midchord. With further increases in angle of attack, the separation moves rapidly forward to the vicinity of the leading edge, so that at about 20°, most of the upper surface is stalled.

The S809 profile was developed using the Eppler design code (Eppler and Somers, 1980a, 1980b). Consequently, the surface profile is defined by a table of coordinates rather than by an analytical expression. To obtain the fine resolution needed for our numerical simulations, we interpolated between the defining surface coordinates using a cubic spline.

CFD Code

Since we could examine only one code, we wanted a code with capabilities that were more or less representative of most commercial CFD codes. We looked for the capability to calculate incompressible, laminar/turbulent, 2-D/3-D, steady/unsteady flows, and to run on desk-top workstations. For our calculations, we used a SUN SPARC-10. Resource constraints forced us to look at codes that were currently licensed for Sandia's computing facilities. We made no effort to find the "best" CFD code for wind turbine applications.

Based on these criteria and constraints, we selected CFD-ACE for our studies. CFD-ACE is a computational fluid dynamics code that solves the Favre-averaged Navier-Stokes equations using the finite-volume approach on a structured, multi-domain, non-overlapping, non-orthogonal, body-fitted grid (CFDRC, 1993). The solution algorithms are pressure based. The code can solve laminar and turbulent, incompressible and compressible, 2-D and 3-D, steady and unsteady flows. Several turbulence models are available, including Baldwin-Lomax, Launder and Spalding k-ε, Chien low-Reynolds number k-ε, RNG[1] k-ε, and k-ω. The default model is Launder and Spalding k-ε. During this investigation, we experienced problems with the k-ω model. CFDRC was able to duplicate our results and began an effort to identify and fix the problem. The k-ω model, therefore, was not available for this study. CFD-ACE has the capability to handle domain interfaces where the number of cells in adjacent domains are not equal, although each cell in the coarser-grid domain must exactly interface with an integer number of cells in the finer-grid domain. This capability was used in our simulations of mixed laminar/turbulent flow.

[1] Re-Normalization Group

Numerical Results

Our initial CFD simulations used a C-type grid topology with approximately 300 cells along the airfoil's surface and 24 cells normal to the surface. The normal grid spacing was stretched so that the cell thickness at the surface gave $y^+ \geq 30$. In the streamwise direction, the wake was modeled with 32 cells. The computational domain extended to 10 chord lengths from the body in all directions. Fully turbulent flow was assumed using the default k-ε turbulence model. All calculations were made at a Reynolds number of 2×10^6.

Figures 2 through 4 show comparisons between the calculated and experimental surface pressure distributions for angles of attack of 0°, 1.02°, and 5.13°, respectively. The C_p comparisons for 0° and 1° show reasonably good agreement over the entire airfoil surface, except in the regions of the laminar separation bubbles. The experimental pressure distributions show the laminar separation bubbles just aft of the midchord on both the upper and lower surfaces. They are indicated by the experimental data becoming more-or-less constant with respect to x/c, followed by an abrupt increase in pressure as the flow undergoes turbulent reattachment. Since the calculations assume fully turbulent flow, no separation is indicated in the numerical results. Figure 4 shows that the pressure comparison for 5° is good except over the forward half of the upper surface. Here the calculation is not adequately capturing the suction-side pressure.

Table 1 compares the aerodynamic coefficients for these same cases. The predicted lift coefficients are accurate to within 10% and the moment coefficients to within 16%. The predicted drag coefficients are between 50% and 80% higher than the experiment results. This overprediction of drag was expected since the actual airfoil has laminar flow over the forward half.

Before proceeding with calculations at higher angles of attack, we made a more detailed analysis of the errors in the calculated pressure on the forward half of the upper surface for 5° angle of attack. We ran calculations with all of the available turbulence models and tried several grid refinements, especially around the nose. The results were essen-

Nomenclature

c	chord	m	pitch moment	y^+	dimensionless sublayer distance from wall = $u_\tau y/\nu$
C_d	drag coefficient = d/qS	p	pressure		
C_l	lift coefficient = l/qS	p_∞	freestream reference pressure	α	angle of attack
C_m	moment coefficient about $0.25c$ = m/qcS	q	dynamic pressure = $\rho U_\infty^2/2$	ν	kinematic viscosity
		U_∞	freestream velocity	ρ	density
C_p	pressure coefficient = $(p-p_\infty)/q$	u_τ	friction velocity = $\sqrt{\tau_w/\rho_w}$	ρ_w	density at wall
d	drag	x	axial coordinate from nose	τ_w	wall shear stress
l	lift	y	normal coordinate from meanline		

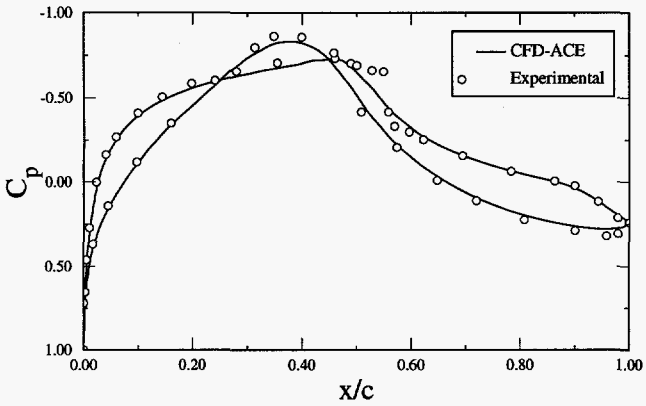

Figure 2. Pressure Distribution for $\alpha = 0°$, Fully Turbulent Calculation

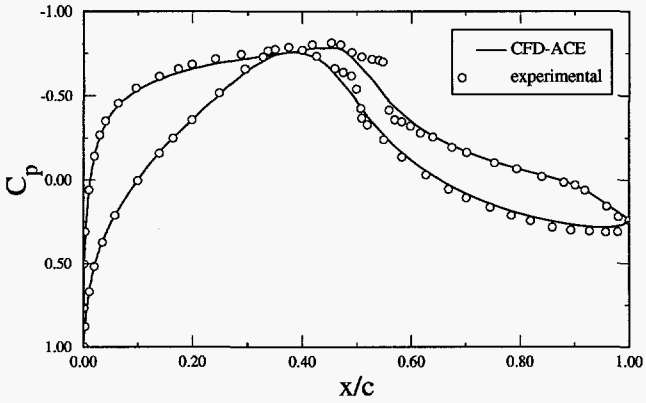

Figure 3. Pressure Distribution for $\alpha = 1.02°$, Fully Turbulent Calculation

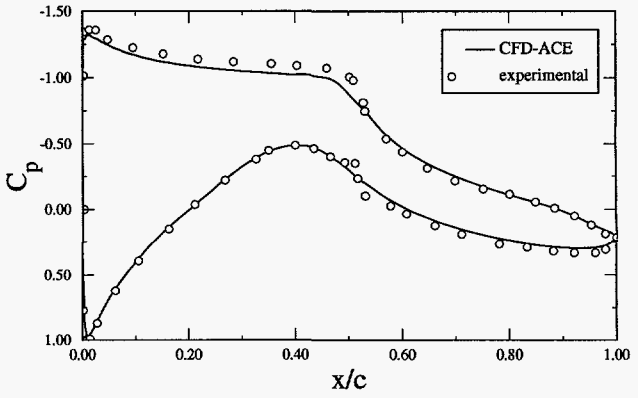

Figure 4. Pressure Distributions for $\alpha = 5.13°$, Fully Turbulent Calculation

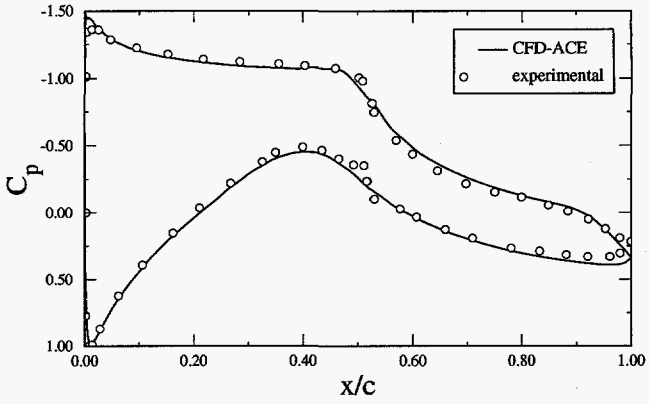

Figure 5. Pressure Distribution for $\alpha = 5.13°$, Euler Calculation

tially the same as those shown in Figure 4. To check the effects of the fully turbulent flow assumption, we also ran an Euler calculation at this angle of attack. The results are shown in Figure 5. This comparison shows very good agreement over the forward half of both the upper and lower surfaces, indicating that the disagreement in Figure 4 is a result of assuming turbulent flow over the forward half of the airfoil. The pressure at the tail of the airfoil shows some error because the effect of the thickening boundary layer is not captured. We tried running a fully laminar calculation, but could not get a converged solution. The laminar flow separated on both surfaces at approximately the 50% chord positions, but because there was no turbulence model, it was unable to transition and reattach as occurs in the actual flow.

Table 1. Comparisons Between Calculated and Experimental Aerodynamic Coefficients, Fully Turbulent Calculations

α deg	C_l				C_d				C_m			
	calc	exp	error $\times 10^4$	% error	calc	exp	error $\times 10^4$	% error	calc	exp	error $\times 10^4$	% error
0	0.1324	0.1469	-145	-10	0.0108	0.0070	38	54	-0.0400	-0.0443	43	-10
1.02	0.2494	0.2716	-222	-8	0.0110	0.0072	38	53	-0.0426	-0.0491	65	-13
5.13	0.7123	0.7609	-486	-6	0.0124	0.0070	54	77	-0.0513	-0.0609	96	-16

After some thought and consultation with the staff at CFDRC, we decided that what was needed was the ability to simulate a mixture of both laminar and turbulent flow, i.e., we needed a good transition model in the code. This would allow us to more accurately predict the surface pressure and greatly improve the drag predictions. Unfortunately, we know of no good production transition models with universal applicability. To the best of our knowledge, no commercial CFD code contains a transition model. CFDRC agreed to add the capability to run mixed laminar and turbulent flow by splitting the computational region into different domains and specifying laminar flow within certain domains. The remaining domains use the standard k-ε turbulence model. The disadvantages of this approach are that the accuracy of the simulation depends on one's ability to accurately guess the transition location, and a new grid must be generated if one wants to change the transition location.

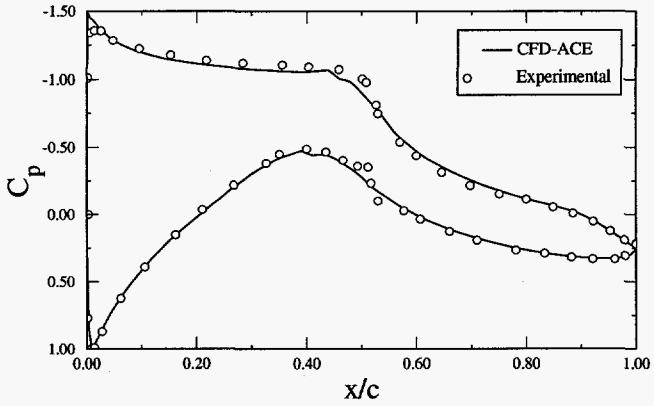

Figure 6. Pressure Distribution for $\alpha = 5.13°$, Mixed Laminar/Turbulent Calculation

Figure 6 shows the comparison for surface pressure at $\alpha = 5.13°$ with this mixed laminar/turbulent model. This simulation used 324 cells along the airfoil surface and 32 cells normal to the surface in the laminar domain. The spacing normal to the wall was stretched to give $y^+ \leq 5$ in the laminar region and $y^+ \geq 30$ in the turbulent regions. This change in the cell thickness at the wall is necessary because laminar flow is calculated up to the wall, while turbulent flow using the k-ε turbulence model uses wall functions within the cell at the wall. The transition locations on both the upper and lower surfaces were specified at the locations of maximum thickness as measured from the mean line, $x/c = 0.45$ on the upper surface and $x/c = 0.40$ on the lower surface. The "wiggles" in the calculated pressure curves at these points are an artifact of the domain interface where four cells in the laminar domain interface with one cell in the turbulent domain.

The pressure coefficients are in very good agreement over the full airfoil surface, except for a small region on the upper-surface leading edge where the pressure is underpredicted. We believe that this is due to a small inaccuracy in the leading edge radius. The table of defining surface coordinates (Somers, 1989) does not give sufficient definition of the S809 leading edge to accurately duplicate the leading edge radius of the experimental model. Table 2 shows the comparison of the aerodynamic coefficients. At 5°, the lift coefficient is now equal to the experimental value. The pitch moment has a 4% error, and the error in the calculated drag has been reduced to 1%. The errors in the coefficients at 0° and 1° have also been significantly reduced. These angles of attack were rerun using the same grid as for the 5° case.

Figures 7 through 9 show the pressure distributions for angles of attack of 9.22°, 14.24°, and 20.15°, respectively. For these angles of attack, the upper-surface transition point was moved forward to the leading edge. The lower-surface transition point remained at $x/c = 0.40$. For 20.15°, the simulations were run fully turbulent. For 9.22°, the computed pressure distribution agrees well with the experiment except for approximately the last 10% of the trailing edge. The experimental data show that there is a small separation zone on the upper surface in this region. This separation was not predicted by the simulation. At 14.24° and 20.15°, there is considerable difference between the experimental and numerical results. The experimental data show that at 14.24° the aft 50% of the upper surface has separated flow. The calculations predict separation over only the aft 5%. At 20.15°, the flow is separated over most of the upper surface. The calculations predict separation on only the aft 50%.

These discrepancies between the experimental data and the calculations are also reflected in the aerodynamic coefficients in Table 2. Figures 10 through 12 compare the numerical and experimental lift, drag, and moment coefficients, respectively. The calculated lift coefficients are accurate through approximately 9° angle of attack. Above this angle, the calculations do not pick up the airfoil's stall behavior and, therefore, overpredict the lift. The drag and pitch moment show similar behavior. The accuracy of the calculated pitching moment at $\alpha = 14.24°$ and the drag at $\alpha = 20.15°$ are more accidental than due to accurate modeling of the flow.

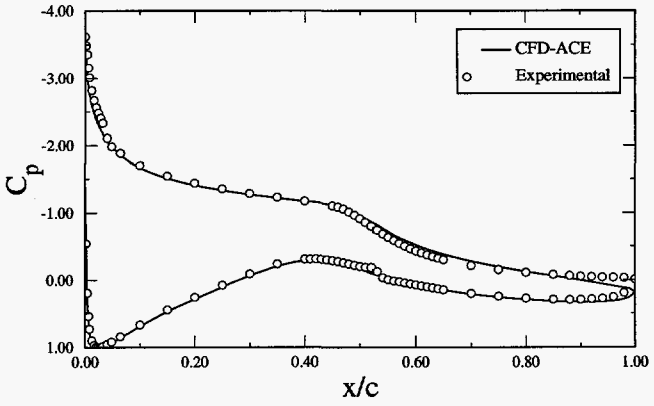

Figure 7. Pressure Distribution for $\alpha = 9.22°$, Mixed Laminar/Turbulent Calculation

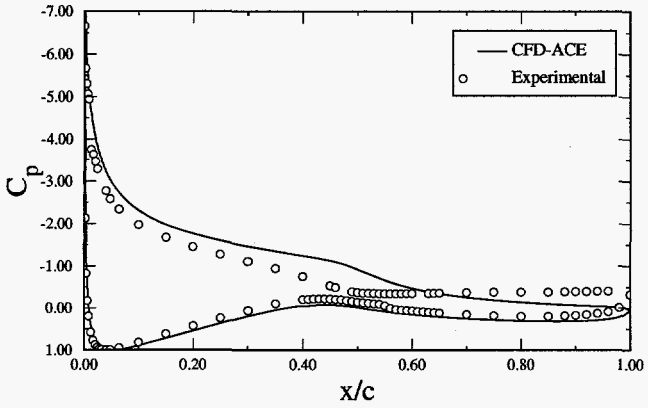

Figure 8. Pressure Distribution for $\alpha = 14.24°$, Mixed Laminar/Turbulent Calculation

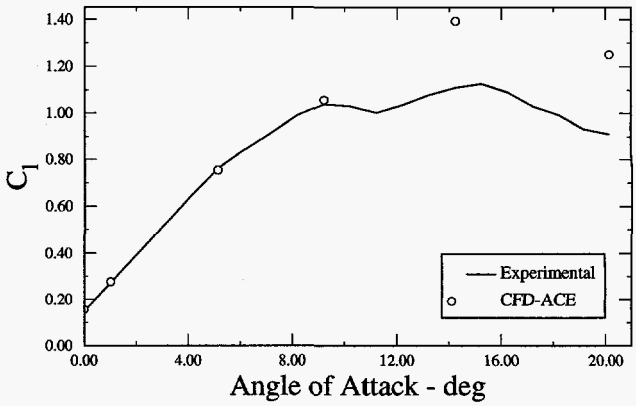

Figure 10. Lift Coefficients

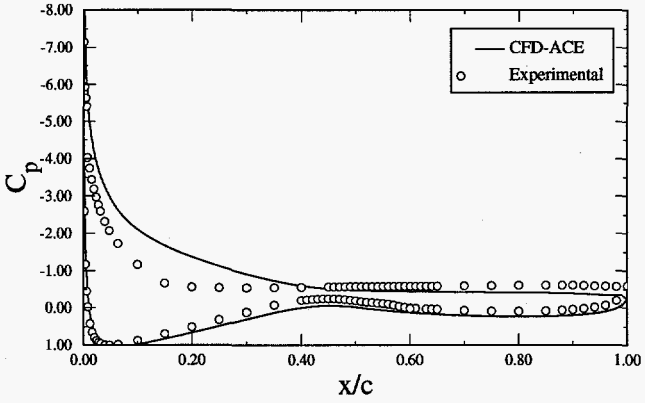

Figure 9. Pressure Distribution for $\alpha = 20.15°$, Fully Turbulent Calculation

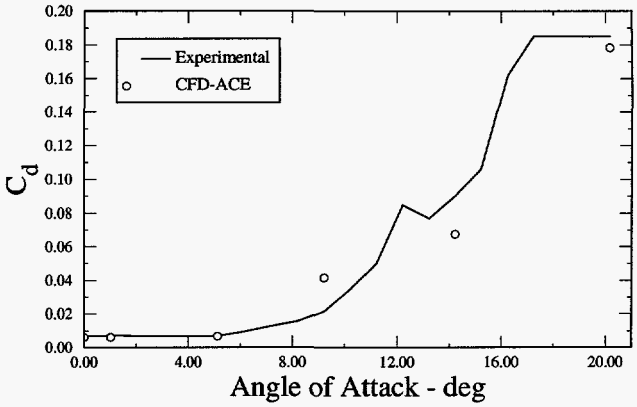

Figure 11. Drag Coefficients

Table 2. Comparisons Between Calculated and Experimental Aerodynamic Coefficients, Mixed Laminar/Turbulent Calculations

α deg	C_l				C_d				C_m			
	calc	exp	error $\times 10^4$	% error	calc	exp	error $\times 10^4$	% error	calc	exp	error $\times 10^4$	% error
0	0.1558	0.1469	89	6	0.0062	0.0070	-8	-11	-0.0446	-0.0443	-3	1
1.02	0.2755	0.2716	39	1	0.0062	0.0072	-10	-14	-0.0475	-0.0491	16	-3
5.13	0.7542	0.7609	-67	-1	0.0069	0.0070	-1	-1	-0.0586	-0.0609	23	-4
9.22	1.0575	1.0385	190	2	0.0416	0.0214	202	95	-0.0574	-0.0495	-79	16
14.24	1.3932	1.1104	2828	25	0.0675	0.0900	-225	-25	-0.0496	-0.0513	17	-3
20.15	1.2507	0.9113	3394	37	0.1784	0.1851	-67	-4	-0.0607	-0.0903	396	-33

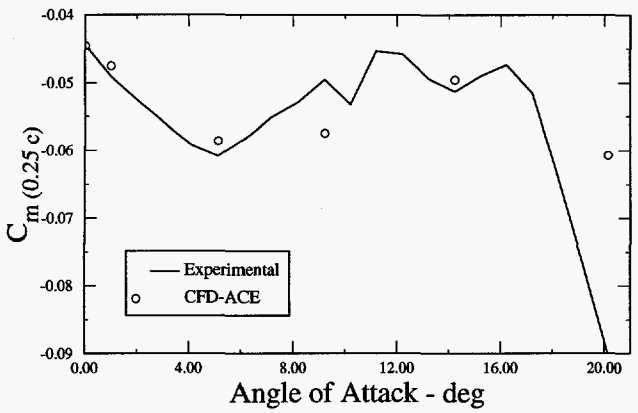

Figure 12. Moment Coefficients About 0.25c

Summary and Conclusions

This paper gives a progress report of our investigation into the capabilities and accuracy of a typical commercial computational fluid dynamics code to predict the flow field and aerodynamic characteristics of wind-turbine airfoils. We have identified two areas in CFD that require further investigation and development in order to enable accurate numerical simulations of flow about current generation wind-turbine airfoils: transition prediction and turbulence modeling.

It must be noted that the calculations presented in this paper were not blind calculations. We knew a priori the transition location from the experimental data and placed the computational transition as close as possible, consistent with numerical stability, to the actual locations. What these calculations show is that accurate predictions of the aerodynamic coefficients for attached flow are possible if one knows where the flow transitions. In an actual design environment, however, the designer would not know a priori the transition location, and would, therefore, need to make a reasonably accurate guess. This requires a designer with aerodynamic experience. What is really needed is an accurate, universally applicable transition model.

Horizontal axis wind turbines routinely operate in the post-stall regime, so accurate predications in this area are important. While this is a dynamic environment rather than a static one, we consider accurate static calculations a prerequisite to accurate dynamic calculations. We have shown that the default turbulence model in most CFD codes, the k-ε model, is not sufficient for accurate aerodynamic predictions at angles of attack in the post-stall region. This is understandable when one considers that the k-ε model uses wall functions based on the law of the wall and that the law of the wall does not hold for separated flows (Wilcox, 1994). We intend to examine the k-ω model for these flow conditions when it becomes available in CFD-ACE. However, considering that turbulence is an ongoing research area, it's not clear that any existing model will work well for this flow regime.

Acknowledgments

The authors which to thank James Tangler of the National Renewable Energy Laboratory and Robyn Reuss Ramsay of Ohio State University for their assistance in obtaining the S809 wind tunnel data, and Mark Rist of CFD Research Corporation for his assistance with CFD-ACE.

References

CFDRC, 1993, *CFD-ACE Theory Manual*, ver. 1.0, CFD Research Corp., Huntsville, AL.

Eppler, R, and D. M. Somers, 1980a, "A Computer Program for the Design and Analysis of Low-Speed Airfoils," NASA TM-80210.

Eppler, R, and D. M. Somers, 1980b, "Supplement To: A Computer Program for the Design and Analysis of Low-Speed Airfoils," NASA TM-81862.

Somers, D. M., 1989, "Design and Experimental Results for the S809 Airfoil," Airfoils, Inc., State College, PA

Wilcox, D. C., 1994, *Turbulence Modeling for CFD,* DCW Industries, Inc., La Cañada, CA, pp. 126-128.